Effects of data point distribution and mathematical model on finding the best-fit sphere to data

P. Bourdet, C. Lartigue, and F. Leveaux
Laboratoire Universitaire de Recherche en Production Automatisée, Ecole Normale Supérieure de Cachan, Cachan, France

Probe calibration on a coordinate measuring machine is dependent on the accuracy with which the center of a reference sphere can be located. In this article, a theoretical model for sphere is fitted to a set of sampled surface points using the least-squares criterion. An analysis is conducted of various errors involved during the steps leading to the identification of the sphere and location of its center. The errors include those associated with surface accessibility for sampling, points sampling strategies, optimization algorithm, and probe diameter versus reference sphere diameter. Inferences are drawn regarding the relative influence of these errors, and a calibration strategy is proposed as a function of sampled points, optimization algorithm, and the geometric surface involved.

Keywords: *Coordinate measuring machine; probe calibration; uncertainty*

Introduction

The inspection of mechanical parts using a coordinate measuring machine (CMM) requires the use of several probes with different dimensional characteristics. The calibration of these probes involves the measurement of a reference sphere, the center of which represents the origin of the measurement coordinate system. The choice of the measured points on the spherical surface and the optimization algorithm used to fit a geometrical model to the sphere result in a center location error. This error affects the results of all subsequent measurements.

The aim of this article is to estimate this error when the probe calibration is performed by measuring a portion of the reference sphere (*Figure 1*).

A simulation model is used to evaluate the error made during identification of the geometric element involved, and an experimental study is conducted to validate simulation results.

Finally, a calibration procedure is proposed that improves the accuracy with which the sphere center is located and thus, overall probe calibration.

Address reprint requests to P. Bourdet, Laboratoire Universitaire de Recherche en Production Automatisée, Ecole Normale Supérieure de Cachan, 61 Avenue du Président Wilson, 94235 Cachan Cedex, France.

Sphere identification by the least-squares criterion

An optimized theoretical model is fitted to the set of n points sampled from the real surface.[1,2] In this article, the commonly used least-squares criterion is used.

The optimization method involves the minimization of the quadratic sum $W = \sum_{i=1}^{n} d_i^2$, where d_i is the deviation between measured points and the optimized surface. An optimum solution is reached when the p parameters that define the p order surface involved are computed.[3] For a sphere, four parameters are required: three parameters (u, v, w) for center location and one δr for the radius.

The surface is represented by a set of n points $\Omega_i(x_i, y_i, z_i)$ in the CMM coordinate system $\mathcal{R}(O; \vec{x}, \vec{y}, \vec{z})$. Those points represent the center of the spherical probe (radius r) in contact with the spherical reference surface, radius R (*Figure 1*). The associated sphere is thus computed step by step as follows[1,4]:

First step

Using four points belonging to the set of measured points Ω_i, an ideal nominal sphere close to the solution is computed. $O'(x_o, y_o, z_o)$ denotes the nominal sphere center and R_0 its radius.

Using a transformation, the measured points are expressed in $\mathcal{R}'(O'; \vec{x}, \vec{y}, \vec{z})$ to obtain the set

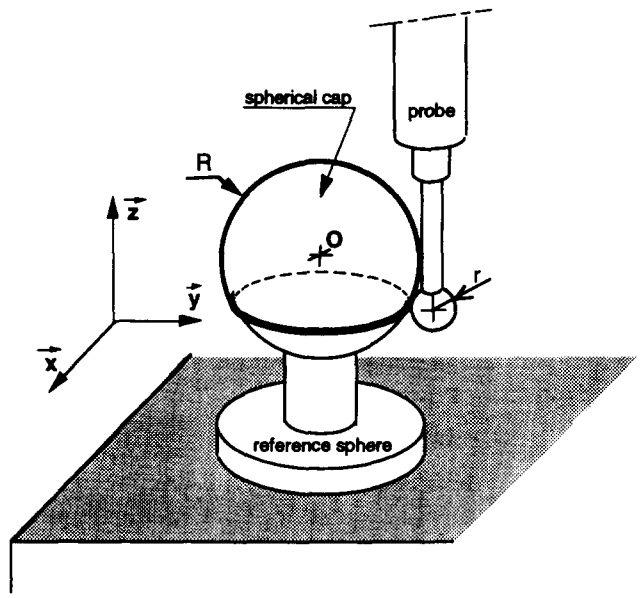

Figure 1 Spherical cap measured by CMM probe

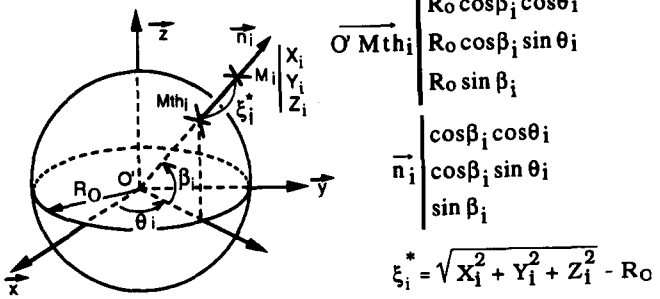

Figure 2 Ideal nominal sphere

$M_i(X_i; Y_i; Z_i)$ with $X_i = x_i - x_o$; $Y_i = y_i - y_o$ and $Z_i = z_i - z_o$.

Second step

For each point M_i, the corresponding theoretical point Mth_i on the ideal nominal sphere, the normal $\vec{n}_i$ and deviation ξ_i^* are computed (*Figure 2*).

Third step

In this step, a small displacement $\vec{D}_{Mthi}$ of each theoretical point *Mthi,* and a small variation of the radius δr are applied to the nominal sphere. Then, the deviations *ei* are defined by Equation (1):

$$e_i = \xi_i^* - (\vec{D}_{Mthi} \cdot \vec{n}_i) - \delta r \quad (1)$$

$\vec{D}_{Mthi}$ is expressed using the displacement of the center $\vec{D}_O(u, v, w)$ and:

$$e_i = \xi_i^* - (u \cos\beta_i \cos\theta_i + v \cos\beta_i \sin\theta_i + w \sin\beta_i + \delta r) \quad (2)$$

The least-squares method is used to find $U(u, v, w, \delta r)$, which minimizes the sum of squares of the deviations e_i.

The problem is more conveniently formulated as the solution to the linear system:

$$A \cdot U = B \quad (3)$$

where the matrix A and B are given in Appendix A.

The fitted sphere is then known in the CMM coordinate system $\mathcal{R}$ by its center: $O^*(X_o^*, Y_o^*, Z_o^*)$, with $X_o^* = x_o + u$; $Y_o^* = y_o + v$; $Z_o^* = z_o + w$, and its radius $R^* = R_o + \delta r$.

The radius R^* represents the sum of the radius R of the spherical reference surface and of the radius r of the spherical probe.

Validation step

The following quantities are computed:

- the deviations d_i between the measured points on the spherical surface and the best fitting sphere

$$d_i = \sqrt{(x_i - X_0^*)^2 + (y_i - Y_0^*)^2 + (z_i - Z_0^*)^2} - R^*$$

- the optimized deviations e_i given by Equation (2)
- the criterion of the small displacements $\varepsilon_i = d_i - e_i$

The result is validated if $\varepsilon_i \leq 10^{-2}\,\mu$m. If not, another optimization must be performed using the best fitting sphere as the new nominal sphere.

Uncertainty in identified surface parameters

Evaluation of errors in the parameters

Using CMM data, the methodology described previously leads to an optimum solution based on the least-squares criterion. However, regardless of the CMM or reference sphere used, CMM data are never error free, and the small uncertainty associated with the position of each sampled point leads to an uncertainty in the position of the center of the reference sphere. The computations performed during the optimization procedure amplify this uncertainty. This error amplification is influenced by the number of sampled points, their location on the spherical surface, and the error inherent in the measurements returned. An evaluation of the quality of the results returned can be undertaken.

A first estimate can be obtained by computing the condition number of matrix A[5,6]:

$$\kappa(A) = \text{cond}(A) = \|A\|\|A^{-1}\| \quad (4)$$

where A^{-1} denotes the inverse of matrix A and $\|\cdot\|$

a matricial norm. This number evaluates the sensitivity of the solution U of the linear system in Equation (3) with respect to the variation in the data.

A linear system for which $\kappa(A) \gg 1$ is called ill conditioned, and a linear system for which $\kappa(A) \cong 1$ is called well conditioned.[5,6]

Additional information about the condition number is developed in Appendix B.

Computation of the covariance matrix could complete this approach and provide an estimate of the standard deviation of the results.[6,7] This approach was developed for the circle by MacCool.[8] Lotze has estimated the uncertainty of the parameters and the form element itself using random error propagation. He concluded that "each extrapolation area far from measured points provide a great error magnification."[9]

Forbes has evaluated numerical stability of different algorithms for finding least-squares best fit sphere to data using statistical methods.[10] Particularly, he showed that the linear least-squares fitting algorithms work well for data scattered over a great spherical cap, but become unstable for near planar data.

A numerical method (not statistical) that evaluates the error of optimized parameters and thus the uncertainty in the center location of the measured sphere is proposed.

The reference sphere is assumed to be known. Simulated points are generated by adding an error to points on the surface of the perfect sphere.

We characterize the error associated with a point M_i by a deviation ξ_i along the normal to the sphere.

This deviation includes all possible error sources: geometrical errors of the CMM, the resolution of the scales, probe technology, and the measurement direction of the probe.

ξ_i takes on any value between two limiting values:

$$\xi_i\text{min} \leq \xi_i \leq \xi_i\text{max}$$

As the spherical surface is defined by n points, a total of 2^n spheres can be identified by the algorithm previously described, where for each sphere, the set (ξ_i) $1 \leq i \leq n$ is a combination of $\xi_i$max and $\xi_i$min.

For each sphere j, $1 \leq j \leq 2^n$ the $(uj, vj, wj, \delta rj)$ parameters are computed according to the previously described algorithm. The origin of the CMM coordinate system is the reference sphere center and Ecj, defined by Equation (5), represents the error of location of the sphere center:

$$Ecj = (X_{oj}^{*2} + Y_{oj}^{*2} + Z_{oj}^{*2})^{1/2} \quad (5)$$

The maximum deviation is defined by

$$Ecmax = \max \{Ecj\}\ 1 \leq j \leq 2^n \quad (6)$$

Generally, the best estimates of the parameters are obtained when sampled points form a symmetric pattern and are uniformly scattered over the surface of the sphere.

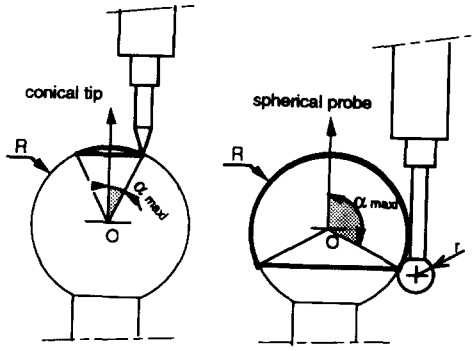

Figure 3 Spherical cap defined by angle α

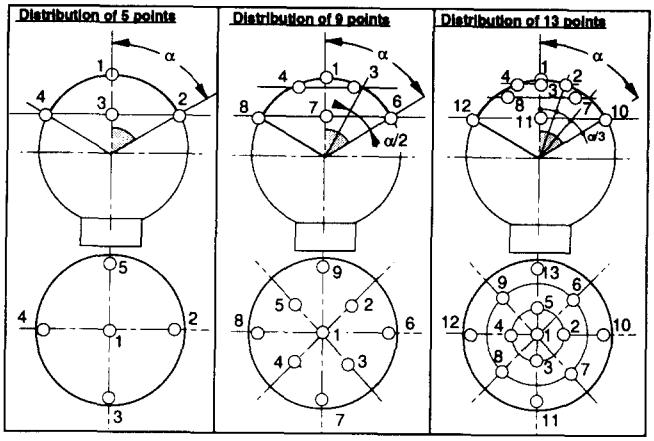

Figure 4 Distribution of points on the spherical cap for a given value α

However, a single probe with conventional X, Y, Z motion cannot access all areas of the spherical surface, and sampling will usually be restricted to a spherical cap defined by an angle α (*Figure 3*). For a probe with a conical tip ($r < 0.02$ mm), this angle is limited to $\alpha = 15°$. In addition, spherical features found on mechanical parts often come in the form of a portion of a sphere. Clearly, the problem posed by the identification of a sphere using n points sampled over a spherical cap must be studied.

Simulation results: computation of the error Ec*max*

The simulations are performed with five, nine, and 13 points scattered as shown in *Figure 4:*

- one on the top of the spherical cap
- the rest, in sets of four points, on several parallel planes.

These distributions of points are commonly used in calibration procedures.

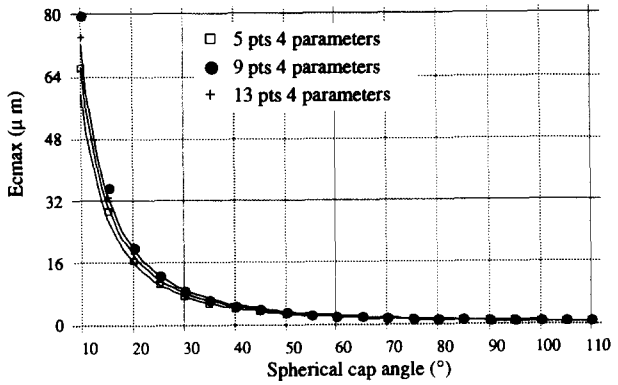

Figure 5 Simulation of the error *Ec*max in function of the number of sampled points

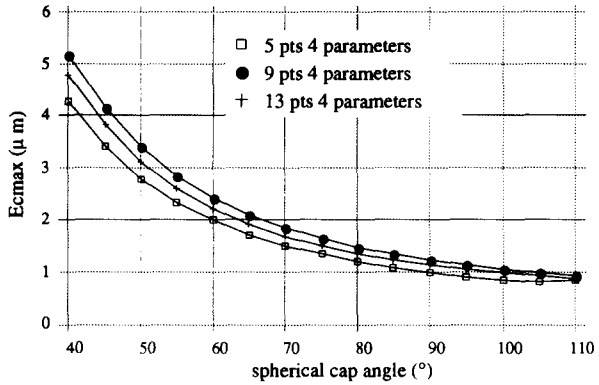

Figure 6 *Ec*max for $\alpha > 40°$

The reference sphere radius is $R = 10$ mm and that of the probe is $r = 1$ mm.

The computation of *Ec*max [Equation (6)] was performed for different values of angle α.

In order to obtain an upper bound of the error *Ec*max, we suppose in the simulations that $\xi_i$max and $\xi_i$min are constant for all points: $\xi_{max} = 1$ μm, ξmin $= 0$ μm.

Notice that, because of the definition of ξ_i along the normal to the sphere, only the value of $\Delta\xi = \xi\text{max} - \xi\text{min}$ influences the value of the maximum error of location of the sphere center *Ec*max.

Because of the linearity of Equation (3), *Ec*max could be evaluated for any value of $\Delta\xi$ different from 1 μm.

Figures 5 and 6 show that, regardless of the number of points, for $\alpha \geq 50°$ *Ec*max values are very close and vary between 3.5 μm ($\alpha = 50°$) and 1 μm ($\alpha = 110°$).

For $\alpha < 50°$, *Ec*max values increase exponentially up to 80 μm. Therefore, probe calibration through measurement of a spherical cap defined by $\alpha < 50°$ is unsuitable.

Notice that the result does not improve when the number of measured points is increased. Results are better for five points because the set of five points is included in the nine and 13 points distribution (*Figure 4*), and due to the algorithm, the supplementary points lead to a greater error in the location. The simulations with nine and 13 points distribution cannot be compared. Effectively, the set of nine points is not included in the set of 13 points.

Table 1 $Ec\text{max} = k_1 \cdot \Delta\xi \cdot \alpha^{k_2}$

Points number	k_1	k_2
5	4,302	1.860
9	5,199	1.859
13	4,715	1.853

Each curve can be approximated by a function of the form $Ec\text{max} = k_1 \cdot \Delta\xi \cdot \alpha^{k_2}$, where k_1 and k_2 depend on the number of the sampled points (*Table 1*).

A study of the condition number confirms the previous observations. In fact, for five, nine, and 13 points, *Table 2* shows that for the smallest values of α, the magnitude of the relative solution error can be 10^2 or 10^4 times higher than that of the relative data error. In this case, the system is ill conditioned. On the other hand, the system is well conditioned for the highest values of α. This is similar to Forbes's result.

The computation of the covariance matrix gives an estimate of the standard deviations of the parameters (u, v, w, δr), but, for the smallest values of α, this does not provide precise information. The study of the correlation matrix shows that, due to the points distribution (scattered symmetrically with respect to the z-axis) the parameters w and δr are strongly dependent, especially for the smallest values of α. MacCool provided a similar result for the circle.[8]

The results of the simulations show that five points distributed as shown in *Figure 4* are sufficient to adequately measure a reference sphere. However, accurate location of the center of a spherical cap defined by $\alpha < 50°$ is not possible. Experimentation confirms this result.

Experimentation and comparative evaluation

Measurement of a sphere defined by a spherical cap. A reference sphere with a radius $R = 10$ mm was measured on a CMM with five and nine points scattered according to *Figure 4*.

The measurement directions are coincident with the CMM axis (x, y, z). For a given point on the sphere, this measurement axis is chosen closest to the normal of the sphere at this point.

The maximum value of the spherical cap that

Table 2 Condition number: four parameters algorithm

	10°	20°	30°	40°	50°	60°	70°	80°	90°	100°	110°
5 points	27 117	11 952	745	259	113	46	22	11	6.85	4.58	3.51
9 points	3 809	$> 10^5$	1 543	326	135	58	29	16	9.6	6.16	4.3
13 points	66 566	559	932	327	118	70	36	20	11.85	7.58	5.18

could be sampled by the probe used (r = 2 mm) was α = 90°. The minimum value that could be sampled (α = 30°) was imposed by the CMM software.

Each sphere measurement was repeated 50 times for each value of α: 30°, 40° . . . 90°. For the 50 replicate measurements and at each angle α of the spherical cap, the error Ec_k ($1 \leq k \leq 50$) was estimated. An experimental value for *Ec*max was defined as

$$Ecmax_E = \max \{Ec_k\}\ 1 \leq k \leq 50 \qquad (7)$$

Figures 7 and 8 compare simulated and experimental values of *Ec*max. It can be seen that experimental values of $Ecmax_E$ follow the general trend of the simulated ones, and that simulated values obtained with $\Delta\xi$ = 4 μm provide an upper bound for experimental values of *Ec*max. The apparent value of $\Delta\xi$ required to fit the experimental values varies with α. This observation is more readily apparent in the case of nine sampled points (*Figure 8*) and will be explored further in the following sections.

An experimental method used to estimate values of $\Delta\xi$ as a function of the angle α that could be used in the simulations is developed.

This method only requires measurements of a point on a plane surface.

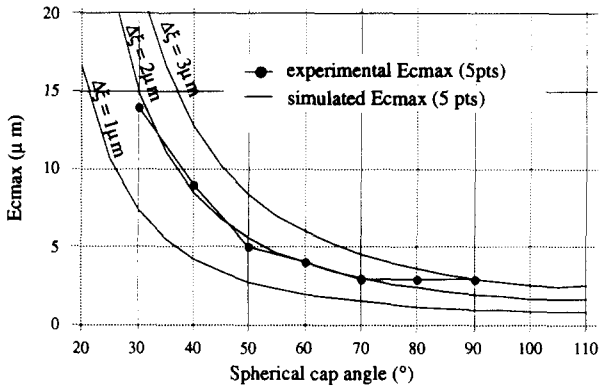

Figure 7 Comparison of simulated and experimental *Ec*max for five probing points

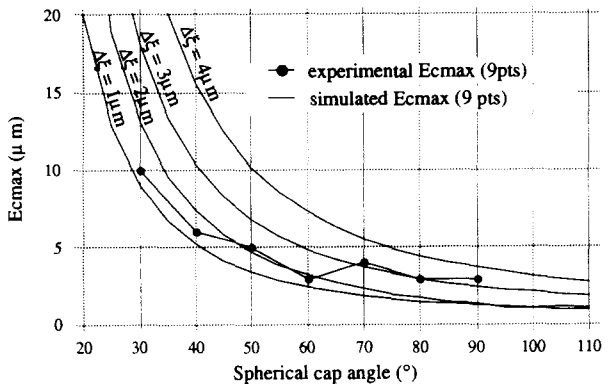

Figure 8 Comparison of simulated and experimental *Ec*max for nine probing points

Experimental estimation of $\Delta\xi$. The error ξ associated with a measured point may be determined experimentally. For this purpose, repeatability tests of a measured point on a plane surface were conducted with a CMM.

The plane surface has orientation angle β as shown in *Figure 9*. β can vary between 0° and 90°. The direction of the probe is the CMM Z-axis.

Two measurement directions are tested: $0° < \beta < 45°$, the direction of the Z-axis, and $45° < \beta < 90°$, the direction of the Y-axis.

For each orientation β, the measurement of the same point M is repeated 50 times. The returned coordinate values of the point are rounded off to

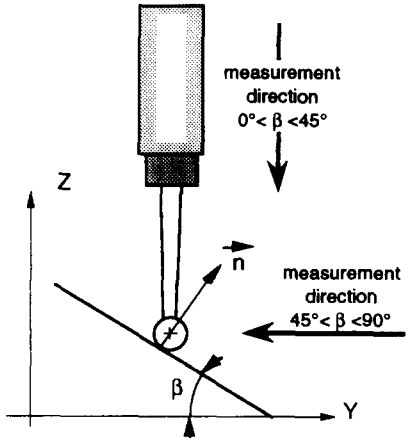

Figure 9 Measurement direction

Table 3 ($\Delta\xi$) evaluated from a measured point on a plane surface

β (°)	0°	5°	10°	15°	20°	25°	30°	35°	40°	45°
Measurement direction: z axis										
$\Delta\xi(\mu m)$	2	1	1.16	1.21	1.3	2.3	2.2	1.1	2.3	2.1
β (°)	45°	50°	55°	60°	65°	70°	75°	80°	85°	90°
Measurement direction: y axis										
$\Delta\xi(\mu m)$	1	1	2.1	1.4	3.6	4	1.2	2	1.4	4

Table 4 Comparison between $(Ec\max)_S$ and $(Ec\max)_E$

α(°)	30°	40°	50°	60°	70°	80°	90°
five probing points							
$(Ec\ \max)_E$ (μm) *Figure 7*	14	9	5	3.9	2.9	2.9	2.9
$(Ec\ \max)_S$ (μm)	16.5	10.5	5.5	4	6.3	2.5	4.5
with $\Delta\xi = \max(\Delta\xi(\beta))E$ where $\beta = \{0;\alpha\}$ *Table 3*	with $\Delta\xi = 2.2$	with $\Delta\xi = 2.3$	with $\Delta\xi = 2$	with $\Delta\xi = 2$	with $\Delta\xi = 4$	with $\Delta\xi = 2$	with $\Delta\xi = 4$
nine probing points							
$(Ec\ \max)_E$ (μm) *Figure 8*	9.7	5.89	4.9	2.8	3.9	2.8	2.8
$(Ec\ \max)_S$ (μm)	13.8	8.6	5.3	3.5	5.4	2	3.6
with $\Delta\xi = \max(\Delta\xi(\beta))E$ where $\beta = \{0;\alpha/2;\alpha\}$ *Table 3*	with $\Delta\xi = 2.2$	with $\Delta\xi = 2.3$	with $\Delta\xi = 2.3$	with $\Delta\xi = 2.2$	with $\Delta\xi = 4$	with $\Delta\xi = 2.3$	with $\Delta\xi = 4$

the micrometer due to the resolution of the scales. Using coordinate values, the values ξ_j $(1 \leq j \leq 50)$ are computed and then $(\Delta\xi)_E$ is determined for each angle β (*Table 3*):

$$(\Delta\xi(\beta))_E = \max\{\xi_j(\beta)\} - \min\{\xi_j(\beta)\} 1 \leq j \leq 50 \quad (8)$$

Simulations using $\Delta\xi_S$ and comparison. Experimental results obtained from measurement of a point on a planar surface (*Table 3*) enable the determination, for a given angle α, of the maximum value, noted $\Delta\xi_S$, corresponding to the set of measured points:

- for five points, $\Delta\xi_S = \max\{\Delta\xi(\beta)\}$, where $\beta \in \{0°, \alpha\}$
- for nine points, $\Delta\xi_S = \max\{\Delta\xi(\beta)\}$, where $\beta \in \{0°, \alpha/2, \alpha\}$

For each value α, $\Delta\xi_S$ is used in the simulations for five and nine points to evaluate the maximum error of location of the sphere center noted $Ec\max_S$.

$Ec\max_S$ and $Ec\max_E$ [evaluated using Equation (7)] are compared in *Table 4* for different values of α. It can be seen that simulated $Ec\max_S$ value is a good estimation of the experimental one.

Therefore, the value $\Delta\xi_S$ evaluated by measuring a point on a planar surface (see previous section) can provide a good approximation of the value $\Delta\xi$, which can be used to simulate the uncertainty in the sphere center location.

Conclusion. The proposed simulations provide a good estimation of the maximum error of location of the sphere center $Ec\max$, which depends on the area of the spherical cap. This supposes the knowledge of the range $\Delta\xi$ that is evaluated by measuring a point on a planar surface with different orientations. But the results obtained with the previous algorithm show that for the smallest values of the angle α, the error of location of the sphere center leads to an unacceptable calibration of the probe.

In order to improve the probe calibration, we propose another mathematical model in which the radius of the reference sphere is assumed to be known. The optimization is only performed on the three parameters $U'(u, v, w)$.

Table 5 Condition number: three parameters algorithm

	10°	20°	30°	40°	50°	60°	70°	80°	90°	100°	110°
5 pts	80.9	19.3	8	4	2.2	1.3	1.2	1.7	2	1.7	1.2
9 pts	117.2	28.6	12.2	6.5	3.8	2.5	1.7	1.4	1	1.12	1.11
13 pts	136.2	33.4	14.3	7.7	4.7	3	2.1	1.6	1.25	1.1	1

Forbes proposed other models for fitting spheres to small caps that do not assume a fixed radius.

Improvement of probe calibration

An attempt is made to define an algorithm used to determine the position of the sphere center with better accuracy.

For this purpose, an optimization on the three small displacement parameters u, v, w is performed assuming that radius R^* is known with an accuracy ΔR^*. For probe calibration, $R^* = R + r$, where r represents the probe radius and R the reference sphere radius.

The problem is now formulated as the solution to the linear system $A' \cdot U' = B'$, where A' is deduced from the matrix A by suppression of the last line and column, and B' is deduced from the vector B by suppression of the last line (see Appendix A).

For small values of α, optimization with three parameters leads to much lower values of the condition number: $\kappa(A) < 10^2$ decreasing rapidly (*Table 5*). On the other hand, correlation matrix shows that parameters are then independent.

Simulation runs with five, nine, and 13 points under the same conditions and $R^* = 11$ mm. *Ec*max values resulting from a simulation with three parameters (u, v, w) are compared in *Figure 10* to those resulting from a simulation with four parameters ($u, v, w, \delta r$) using five sampled points. It is readily seen that fixing the value of the radius improves the location of the sphere center. Under this condition, the value of *Ec*max remains less than 3 μm for $15° < \alpha < 70°$. This result remains valid for sampling with nine and 13 points (*Figures 10 and 11*).

A small variation ΔR of the given radius does not affect the previous result: a variation $\Delta R = 1$ mm ($\Delta R \gg \Delta R^*$) results in a variation of *Ec*max $< 10^{-2}$ μm.

This algorithm is therefore efficient for probe calibration, where the reference sphere center must be determined with the best possible accuracy. It can also be used for identification of spherical surface parts for which the radius is "fixed" by the specifications.

The choice of the best algorithm for a given spherical cap (defined by α) can be defined by a critical value α_C:

- for $\alpha < \alpha_C$, the three parameters algorithm minimizes *Ec*max.
- for $\alpha > \alpha_C$, the four parameters algorithm minimizes *Ec*max.

In this experimental study, the critical value of α is $\alpha_C = 70°$.

Conclusions

The proposed simulation method is general and may be applied to all surfaces defined by points and normals. Regardless of the shape and size of the surface, the simulation provides an estimate of

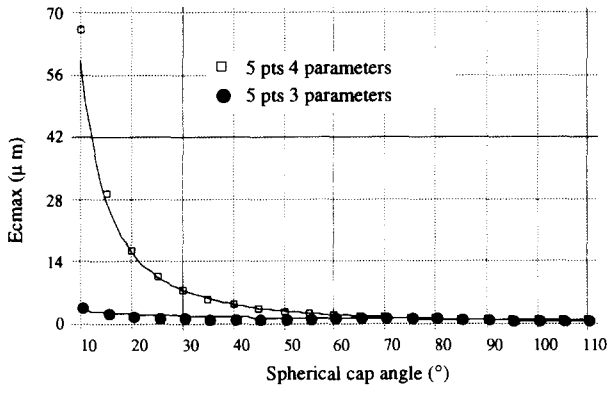

Figure 10 Comparison of simulations using algorithms for optimization over four and three parameters

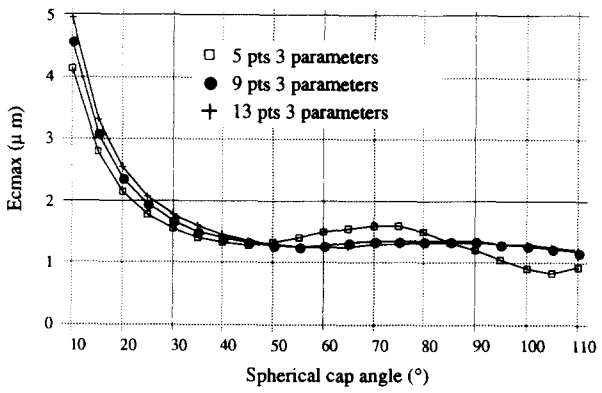

Figure 11 Simulation of the error *Ec*max as a function of the number of sampled points

surface identification accuracy, which depends on the distribution of points.

The method is applied to the sphere in order to evaluate the error of location of a sphere center. This leads to a probe calibration strategy, which is of major interest for CMM metrologists. The numerical simulations show that, due to measurement errors, the sphere center is less well determined when the points are measured on a small spherical cap. This result is nearly insensitive to the number of points (five, nine, and 13 points).

The previous results for small measurement areas is improved by the use of the three parameters model in which the radius of the identified sphere is assumed to be known. The most appropriate model (three or four parameters) for probe calibration on a given spherical cap is given by

- for $\alpha < 70°$, the three parameters algorithm
- for $\alpha \geq 70°$, the four parameters algorithm

In both cases, it is advisable to measure the spherical cap by five points.

References

1 Bourdet, P. and Clément, A. "Controlling a complex surface with a 3 axis measuring machine", *Ann CIRP* 1976, **25**, 354–361

2 Bourdet, P. and Clément, A. "A study of optimal-criteria identification based on small-displacement screw model", *Ann CIRP* 1988, **37**, 503–506

3 Anthony, G. T., Anthony, H. M., Cox, M. G., and Forbes, A. B. "The parametrization of geometric form", Synthesis report contract EUR 13517 EN

4 Bourdet, P. "Contribution à la mesure tridimensionnelle: modèle d'identification des surfaces, métrologie fonctionnelle des pièces mécaniques, correction géométrique des machines à mesurer tridimensionnelles." Thèse d'etat, Université de Nancy I, Nancy, France, 1987

5 Ciarlet, P. G. *Introduction à l'Analyse Numérique Matricielle et à l'Optimisation.* Paris: Masson, 1982

6 Tarantola, A. *Inverse Problem Theory—Methods for Data Fitting and Model Parameter Estimation.* Amsterdam: Elsevier, 1987.

7 Trigeassou, J. Cl. *Recherche de Modèles Expérimentaux.* Paris: Lavoisier, 1988

8 MacCool, J. I. "Systematic and random errors in least squares estimation for circular contours," *Prec Eng* 1979, **1**, 215–220

9 Lotze, W. Precision length measurement by computer-aided coordinate measurement," *J Phys E Sci Instr* 1986, **19**, 495–501

10 Forbes, A. B. "Robust circle and sphere fitting by least squares," Technical Report DITC 153/89, National Physical Laboratory, Teddington, 1989

Appendix A: description of the linear system

The linear system is defined by: $A \cdot U = B$, with

$A = (a_{ij})$

$$\begin{vmatrix} a_{11} & a_{12} & a_{13} & a_{14} \\ a_{12} & a_{22} & a_{23} & a_{24} \\ a_{13} & a_{23} & a_{33} & a_{34} \\ a_{14} & a_{24} & a_{34} & a_{44} \end{vmatrix} \cdot \begin{vmatrix} u \\ v \\ w \\ \delta r \end{vmatrix} = \begin{vmatrix} \sum \xi_i^* \cos \beta_i \cos \theta_i \\ \sum \xi_i^* \cos \beta_i \sin \theta_i \\ \sum \xi_i^* \sin \beta_i \\ \sum \xi_i^* \end{vmatrix}$$

where

$a_{11} = \sum \cos \beta_i^2 \cos \theta_i^2$ $\quad$ $a_{23} = \sum \cos \beta_i \sin \beta_i \sin \theta_i$

$a_{12} = \sum \cos \beta_i^2 \sin \theta_i \cos \theta_i$ $\quad$ $a_{24} = \sum \cos \beta_i \sin \theta_i$

$a_{13} = \sum \cos \beta_i \sin \beta_i \cos \theta_i$ $\quad$ $a_{33} = \sum \sin \beta_i^2$

$a_{14} = \sum \cos \beta_i \cos \theta_i$ $\quad$ $a_{34} = \sum \sin \beta_i$

$a_{22} = \sum \cos \beta_i^2 \sin \theta_i^2$ $\quad$ $a_{44} = n$

Appendix B: condition number

The condition number of matrix A is defined by

$$\kappa(A) = \text{cond}(A) = \|A\|\|A^{-1}\|,$$

where A^{-1} denotes the inverse of matrix A, and $\|\cdot\|$ a matricial norm. This number evaluates the sensitivity of the solution U of the linear system $A \cdot U = B$ with respect to the variation in the data.

Consider the perturbed system $A \cdot (U + \delta U) = B + \delta B$. It can be shown that

$$\frac{\|\delta U\|}{\|U\|} \leq \|A\|\|A^{-1}\| \frac{\|\delta B\|}{\|B\|}$$

This inequality shows that for a given relative data error, the relative solution error increases according to the condition number.

A linear system for which $\kappa(A) \gg 1$ is called ill conditioned, and a linear system for which $\kappa(A) \cong 1$ is called well conditioned.

The mathematical norm used is the L_2 norm, which can be defined by $\|A\|_2 = (\rho(AA^*))^{1/2}$ where A^* denotes the adjoint matrix of A and $\rho(AA^*) = \max_j \lambda_j(AA^*)$ where the terms $\lambda_j(AA^*)$ are the eigenvalues of the matrix AA^*.